

Landau-Zener transitions in a fermionic dissipative environment

Ruofan Chen¹

¹*Science and Technology on Surface Physics and Chemistry Laboratory, Mianyang 621908, China*

(Dated: April 1, 2020)

We study Landau-Zener transitions in a fermionic dissipative environment where a two-level (up and down states) system is coupled to two metallic leads kept with different chemical potentials at zero temperature. The dynamics of the system is simulated by an iterative numerically exact influence functional path integral method. In the pure Landau-Zener problem, two kinds of transition (from up to down state and from down to up state) probability are symmetric. However, this symmetry is destroyed by coupling the system to the bath. In addition, in both kinds of transitions, there exists a nonmonotonic dependence of the transition probability on the sweep velocity; meanwhile nonmonotonic dependence of the transition probability on the system-bath coupling strength is only shown in one of them. As in the spin-boson model, these phenomena can be explained by a simple phenomenological model.

I. INTRODUCTION

In physics and chemistry, it is ubiquitous that a quantum system can be effectively described by two-level systems (TLSs). The simplest example is a particle of total spin $\frac{1}{2}$ under an external magnetic field, which can be called an “intrinsically” two-level system. A more common situation is that a system has continuous degrees of freedom which are associated with a potential with two minima [1, 2]. In 1927, Hund [3] first introduced the quantum tunneling effect when describing the intramolecular rearrangement in ammonia molecules. Soon after, Oppenheimer [4] used the tunneling effect to explain the ionization of atoms in strong electric fields. Since then quantum tunneling in isolated TLSs under external driving has been widely studied. A well-known example is the so-called Landau-Zener problem where an isolated TLS undergoes a time-dependent energy sweep. In such a model, the final transition between states of the TLS is called the Landau-Zener (LZ) transition, which was first solved independently by Landau [5], Zener [6], Stückelberg [7] and Majorana [8] in 1932.

As one of the most fundamental phenomena in quantum physics, the LZ transition plays an important role in various fields such as quantum chemistry [9], atomic and molecular physics [10–12], solid state artificial atoms [13, 14], spin flips in nanomagnets [15, 16], quantum optics [17, 18], Bose-Einstein condensates [19–21], quantum information and computation [22–27], and Landau-Zener-Stückelberg interferometry [28–33].

For isolated TLSs, Landau-Zener transitions can be solved exactly [5–8, 34–36]. However, this is no longer the case when taking the environment into consideration [37–39] except for some limiting cases. How the environment affects the Landau-Zener transition has continuously attracted considerable attentions over the decades. Kayanuma [34] proposed a simple stochastic model having a diagonal energy fluctuating term and gave the analytic LZ transition probability in the rapid fluctuation limit. Gefen *et al.* [37] gave a qualitative indication on how the LZ transition be affected by the environment. Ao and Rammer [38, 39] studied the LZ transition with an Ohmic heat bath and they found that at zero temperature in the limits of very fast and very slow sweeps the transition

probability is the same as in the absence of the bath, which was confirmed by numerical calculations [40, 41]. Wubs *et al.* [24] investigated the influence of a classical radiation field on the LZ transition and obtained analytical results in the limits of large and small frequencies within a rotating wave approximation. Later they [42] gave an exact LZ transition probability for a qubit with linear coupling to a bosonic bath at zero temperature and proposed to use the LZ transition to make qubits as bath detectors. Saito *et al.* [43] studied the LZ transition in a qubit coupled to bosonic and spin bath respectively at zero temperature and discussed their bath-specific and universal behaviors. Nalbach and Thorwart [44] studied the LZ transition in a bosonic dissipative environment by means of an iterative numerically exact influence functional path integral method, and they discover a nonmonotonic dependence of the transition probability on the sweep velocity which can be explained by a simple phenomenological model. Whitney *et al.* [45] found that the Lamb shift of the environment exponentially enhances the coherent oscillation amplitude in the LZ transition. Haikka and Mølmer [46] studied the LZ transition when the system is subjected to continuous probing of the emitted radiation and they found the measurement back action on the system leads to significant excitation. Arceci *et al.* [47] revisited the issue of thermally assisted quantum annealing by a detailed study of the dissipative LZ problem in the presence of a Caldeira-Leggett bath of harmonic oscillators. Huang and Zhao [48] employed the Dirac-Frenkel time-dependent variation to examine dynamics of the LZ problem with both diagonal and off-diagonal qubit-bath coupling.

Till now most studies of the effect of environment on the LZ transition have focused on spin-boson systems where the environment is described as a bath of harmonic oscillators. The effect of a fermionic environment is much less well understood. In this article, we employ an iterative numerically exact influence method [49–52] to study LZ transitions in a fermionic environment where a TLS is coupled to two metallic leads kept with different chemical potentials at zero temperature. Such a method allows us to include nonadiabatic and non-Markovian effects and is well suited for real-time dynamics simulation of quantum dots.

In the pure LZ transition problem, two kinds of transition (from up to down state and from down to up state) proba-

bilities are symmetric. Whether the spin is initially prepared in up state or down state, the final probability that it transits to another state is the same. According to our simulations, this is no longer the case when the system is coupled to the leads. In addition, a nonmonotonic dependence of the transition probability on the sweep velocity exists in both kinds of transition, while nonmonotonic dependence of the system-bath coupling strength is only shown in one of them. These phenomena can be explained by a simple phenomenological model as in the spin-boson model. This nonmonotonic dependence can be understood as a nontrivial competition between relaxation caused by the environment and LZ driving, and it may be useful for optimal control problems.

This article is organized as follows. The details of the model and a quick survey of the method are given in Sec. II. The simulation results and discussions are shown in Sec. III. Finally, some concluding remarks are given in Sec. IV.

II. MODEL AND METHOD

We consider a spin-fermion system with the time-dependent Hamiltonian

$$H(t) = H_S(t) + H_B + H_{SB}, \quad (1)$$

where the system Hamiltonian $H_S(t)$ is the standard LZ Hamiltonian for an isolated TLS for which

$$H_S(t) = \frac{vt}{2}\sigma_z + \frac{\Delta_0}{2}\sigma_x \quad (2)$$

with the tunneling amplitude Δ_0 and the sweep velocity v . Throughout this article we set $\hbar = k_B = 1$ and use dimensionless quantities. The value of Δ_0 is set to $\Delta_0^2 = 0.1$ and the value of v is kept positive. σ_x and σ_z are Pauli matrices, and diabatic states are the eigenstates of σ_z (up $|\uparrow\rangle$ and down $|\downarrow\rangle$ states). When $t \rightarrow \pm\infty$, the diabatic states coincide with the momentary eigenstates of the LZ Hamiltonian.

The bath Hamiltonian H_B describes two independent free fermionic leads ($\alpha = L, R$ for left and right lead) for which

$$H_B = \sum_{\alpha k} \varepsilon_k c_{\alpha k}^\dagger c_{\alpha k}, \quad (3)$$

where the operator $c_{\alpha k}^\dagger$ ($c_{\alpha k}$) creates (annihilates) an electron in the α th lead with state k . These two leads are kept with a chemical potential difference $\Delta\mu$ at zero temperature. Here we suppose the chemical potential of the left lead μ_L is higher than that of the right lead μ_R , and the bandwidth of both leads is taken to be $D = 3$. The middle of the band is set as the zero energy point, and μ_L, μ_R are symmetrically placed on two sides of it, i.e., $\mu_L = \frac{1}{2}(D + \Delta\mu)$ and $\mu_R = \frac{1}{2}(D - \Delta\mu)$.

The system-bath coupling Hamiltonian H_{SB} is taken to be

$$H_{SB} = \sum_{\alpha\beta; kq} V_{\alpha\beta} \sigma_z c_{\alpha k}^\dagger c_{\beta q}, \quad (4)$$

where α, β are the bath indices. With such a system-bath coupling the momentum dependence of the scattering potential is

neglected [52–57]. In particular, only interbath system-bath coupling is under consideration. Here we introduce a control parameter λ of system-bath coupling strength for which $\rho V_{\alpha\beta} = \lambda(1 - \delta_{\alpha\beta})$, where ρ is the density of states of each lead and the factor $(1 - \delta_{\alpha\beta})$ ensures only interbath coupling. Fig. 1 gives a schematic representation of the model.

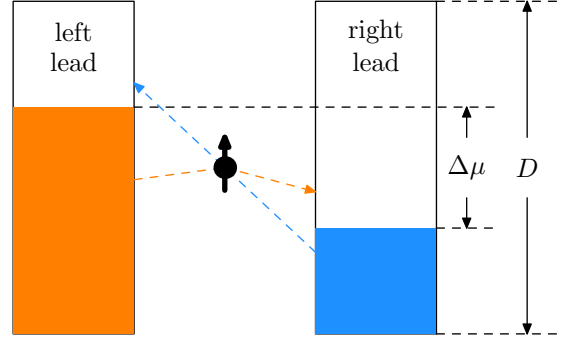


FIG. 1. (Color Online) Scheme of the spin-fermion model. The two leads with bandwidth D are kept with a chemical potential difference $\Delta\mu$ at zero temperature. Electrons in the leads can jump into another lead via and scattered by the spin.

In this article, we employ an iterative numerically exact influence functional path method to investigate the effects of sweep velocity v , system-bath coupling strength λ , and bath chemical potential $\Delta\mu$ on LZ transitions. This method is non-perturbative and allows us to include nonadiabatic and non-Markovian effects, and it is also well suited for real-time dynamics simulations of quantum dots. It was first proposed by Makarov and Makri for the time-independent spin-boson model [49, 50]. Later it was applied to the monochromatically driven spin-boson model [58–61]. It was also adopted to investigate LZ transitions in the spin-boson model [44, 47].

Segal *et al.* generalized this method to the time-independent spin-fermion model by adopting a discretized scheme for tracing out the bath [52, 62–65]. Chen and Xu applied this scheme to study the monochromatically driven spin-fermion model and gave a comparison between the path integral method and the Floquet master equation [57]. This scheme is also adopted in this article. The basic procedure of the path integral method is as follows.

The evolution of total density matrix $\rho(t)$ is given by

$$\rho(t) = U(t)\rho(0)U^\dagger(t), \quad (5)$$

where

$$U(t) = \mathbb{T} \exp \left[-i \int_0^t H(\tau) d\tau \right] = \prod_{t_i=0}^t e^{-iH(t_i)\delta t} \quad (6)$$

with \mathbb{T} being the chronological ordering symbol. Here the product is understood as that the limit is taken over all infinitesimal interval δt between zero and t arranged from right to left in order of increasing time t_i . Employing finite δt approximates the evolution operator $U(t)$ into a product of finite N exponentials for which $U(t) \approx \prod_i T_i$, where $T_i = e^{-iH(t_i)\delta t}$. Now introduce the reduced density matrix of the

system $\rho_S = \text{Tr}_B \rho$ by tracing ρ over the bath degrees of freedom, which is now written as

$$\rho_S(s'', s'; t) = \text{Tr}_B[\langle s'' | T_N \cdots T_1 \rho(0) T_1^\dagger \cdots T_N^\dagger | s' \rangle]. \quad (7)$$

Inserting the identity operator $\int ds |s\rangle\langle s|$ between every two T and relabeling s'', s' as s_N^+, s_N^- gives

$$\begin{aligned} \rho_S(s_N^+, s_N^-; t) &= \int ds_0^+ \cdots ds_{N-1}^+ \int ds_0^- \cdots ds_{N-1}^- \\ &\times \text{Tr}_B[\langle s_N^+ | T_N | s_{N-1}^+ \rangle \cdots \\ &\rho(0) \cdots \langle s_{N-1}^- | T_N^\dagger | s_N^- \rangle]. \end{aligned} \quad (8)$$

The integrand in the above expression is referred as the ‘‘influence functional’’ [52] (IF) which we denote by $I(s_0^\pm, \dots, s_N^\pm)$. The nonlocal correlations in the IF decay exponentially under certain conditions [49], which enables a controlled truncation of the IF. Note that for the spin-fermion system at zero temperature used in this article, the exponential decay is guaranteed by finite $\Delta\mu$ [51, 52]. Therefore the IF can be truncated beyond a memory time $\tau_c = N_s \delta t$ with N_s being a positive integer and the IF can be written approximately as [49, 50, 52, 62, 66]

$$\begin{aligned} I(s_0^\pm, \dots, s_N^\pm) &\approx I(s_0^\pm, \dots, s_{N_s}^\pm) I_s(s_1^\pm, \dots, s_{N_s+1}^\pm) \\ &\times \cdots I_s(s_{N-N_s}^\pm, \dots, s_N^\pm), \end{aligned} \quad (9)$$

where

$$I_s(s_k^\pm, \dots, s_{k+N_s}^\pm) = \frac{I(s_k^\pm, \dots, s_{k+N_s}^\pm)}{I(s_k^\pm, \dots, s_{k+N_s-1}^\pm)}. \quad (10)$$

In order to integrate Eq. (9) iteratively we can define a multiple time reduced density matrix $\tilde{\rho}_S(s_k^\pm, \dots, s_{k+N_s-1}^\pm)$ with initial values $\tilde{\rho}_S(s_0^\pm, \dots, s_{N_s-1}^\pm) = 1$. Its first evolution step is given by

$$\tilde{\rho}_S(s_1^\pm, \dots, s_{N_s}^\pm) = \int ds_0^\pm I(s_0^\pm, \dots, s_{N_s}^\pm), \quad (11)$$

and the latter evolution step is given by

$$\begin{aligned} \tilde{\rho}_S(s_{k+1}^\pm, \dots, s_{k+N_s}^\pm) &= \int ds_k^\pm \tilde{\rho}_S(s_k^\pm, \dots, s_{k+N_s-1}^\pm) \\ &\times I_s(s_k^\pm, \dots, s_{k+N_s}^\pm). \end{aligned} \quad (12)$$

Finally the time-local ($t_k = k\delta t$) reduced density matrix is obtained by

$$\rho_S(t_k) = \int ds_{k-1}^\pm \cdots ds_{k-N_s+1}^\pm \tilde{\rho}_S(s_{k-N_s+1}^\pm, \dots, s_k^\pm). \quad (13)$$

It can be seen that we need to keep track of a $2N_s$ rank ‘‘tensor’’ $\tilde{\rho}_S$ and a $2(N_s + 1)$ rank ‘‘tensor’’ I_s . If the size of the system Hilbert space is M , then a space with size proportional to M^{2N_s} is needed to store $\tilde{\rho}_S$ and a space with size proportional to $M^{2(N_s+1)}$ is needed to store I_s . The space size increases dramatically with increasing M and N_s , which limits the value of time step δt , the length of τ_c and the size

of the system M in a practical calculation. However, because the method is iterative in time it is easy to deal with a time-dependent Hamiltonian.

In principle, the final results of the time-independent model can be extrapolated to the $\delta t \rightarrow 0$ limit and the error brought by finite δt is then eliminated [51, 52]. However, in time-dependent driving case with different δt the driving field is sampled in different time grids, which would bring extra error in extrapolation. In addition, δt can not be arbitrary small with a fixed τ_c since we must ensure that N_s is not too large. Therefore, as in Ref. [57], the extrapolation is not employed in this article.

III. RESULTS AND DISCUSSIONS

In the pure LZ problem, at initial time $t = -\infty$ the system is prepared in one diabatic state, and one seeks the probability P_0 of the system to end up in another at $t = +\infty$. If the system is initially prepared in the up state $|\uparrow\rangle$, which corresponds to the ground state, then P_0 gives the probability of the system to end up in the down state $|\downarrow\rangle$, which now also corresponds to the ground state. In other words, the LZ probability P_0 gives the final probability of the system to stay in the ground state. Similarly, if the system is initially prepared in the down state $|\downarrow\rangle$ then P_0 gives the final probability to stay in the excited state. In summary, P_0 is defined as

$$P_0 = |\langle \uparrow | U_S(\infty, -\infty) | \downarrow \rangle|^2 = |\langle \downarrow | U_S(\infty, -\infty) | \uparrow \rangle|^2, \quad (14)$$

where U_S is the system evolution operator

$$U_S(\infty, -\infty) = \text{T exp} \left[-i \int_{-\infty}^{\infty} H_S(\tau) d\tau \right]. \quad (15)$$

The exact solution for P_0 is given by [5–8]

$$P_0 = 1 - \exp\left(-\frac{\pi\Delta_0^2}{2v}\right). \quad (16)$$

This solution is symmetric for both diabatic states for which whether the system is prepared in the up or down state would not affect the probability of it transiting to another diabatic state.

When the system is coupled to the environment, this symmetry is broken for which the probability of the system staying in the ground or excited state becomes different. For convenience, we denote the LZ probability of the system to stay in the ground state (corresponding to the transition from up to down state) by P_1 , for which

$$P_1 = |\langle \downarrow | U(\infty, -\infty) | \uparrow \rangle|^2, \quad (17)$$

and the LZ probability of the system to stay in the excited state (corresponding to the transition from down to up state) by P_2 , for which

$$P_2 = |\langle \uparrow | U(\infty, -\infty) | \downarrow \rangle|^2. \quad (18)$$

Here U denotes the total evolution operator for which

$$U(\infty, -\infty) = T \exp \left[-i \int_{-\infty}^{\infty} H(\tau) d\tau \right]. \quad (19)$$

In this section the simulation results for P_1 and P_2 are given respectively. In all figures, the simulation results are presented by dots and lines are guides for the eye.

A. Results of P_1

Let us first consider the case where the system is initially prepared in the up (ground) state at $t = -\infty$.

Figure 2 shows the LZ probability P_1 versus sweep velocity v for weak coupling $\lambda = 0.04$ and various $\Delta\mu$. It can be seen that a large velocity regime ($v \gg \Delta_0^2$) can be distinguished from a small velocity regime ($v \ll \Delta_0^2$). The result shown here is similar to that in the spin-boson model for various temperatures [44] for which larger $\Delta\mu$, which can act as a temperature like dephasing contributor [56], suppresses the LZ transition more strongly. In the large-velocity regime ($v \gg \Delta_0^2$), P_1 coincides with P_0 for which little influence of the environment is shown. In the regime where $v < \Delta_0^2$, besides an overall all decrease of P_1 with increasing $\Delta\mu$, a non-monotonic dependence of P_1 on v is shown: with fixed $\Delta\mu$ and decreasing v , P_1 first shows a maximum at v_{\max} , which is smaller than but close to Δ_0^2 , then a minimum at velocity v_{\min} , and finally an increase.

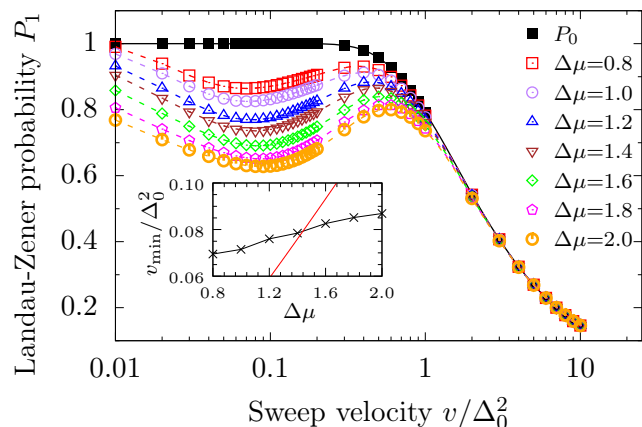


FIG. 2. (Color Online) The LZ probability P_1 versus v for weak system-bath coupling strength $\lambda = 0.04$ and various $\Delta\mu$. Inset: v_{\min} versus $\Delta\mu$ with same λ as in the main figure. The simulation results are shown by black dots, and results by the phenomenological model [Eq. (23)] are shown by the red line.

In the spin-boson model, this nonmonotonicity can not be described by perturbative approaches but can be explained by a simple phenomenological model [44]. Here we give a review on such a phenomenological model. The bath is assumed to mainly induce relaxation. At the initial time the system is prepared in the ground state; therefore only absorption can

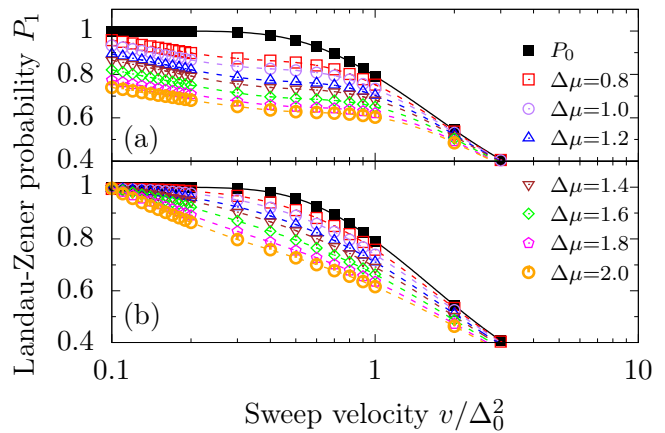


FIG. 3. (Color Online) Same as Fig. 2 for larger system-bath coupling strengths (a) $\lambda = 0.10$ and (b) $\lambda = 0.20$.

occur if an excitation with energy

$$\Delta_t = \sqrt{(vt)^2 + \Delta_0^2} \quad (20)$$

exists in the bath spectrum and thermally populated. The quantity Δ_t varies with time and if it is larger than a threshold energy Δ_c then relaxation would stop. In other words, relaxation can only occur within a time window from $-\frac{1}{2}t_r$ to $\frac{1}{2}t_r$, where

$$t_r = \frac{2}{v} \sqrt{\Delta_c^2 - \Delta_0^2}. \quad (21)$$

The threshold energy Δ_c is taken to be the smaller of the temperature T and the bath cutoff frequency ω_c . Let τ_r denote the system relaxation time; then τ_r must be shorter than t_r for relaxation processes to contribute.

When the sweep velocity v is large, t_r is small for which $t_r \ll \tau_r$; therefore relaxation can not occur and the bath has little influence on the LZ transition for which P_1 coincides with P_0 . In the opposite limit where $v \rightarrow 0$ for which $t_r \gg \tau_r$, the system will get full relaxation at any time according to momentary Hamiltonian. Since relaxation stops at the threshold energy, the system would be adjusted according to Δ_c and T . For small but finite sweep velocity, equilibration is retarded for which the system is relaxed according to the past momentary Hamiltonian. The system is then assumed to be equilibrated toward a time-averaged energy splitting

$$\bar{\Delta}_r = \frac{1}{t_r} \int_{-t_r/2}^{t_r/2} \Delta_t dt, \quad (22)$$

leading to $P_1(v_{\min}) = \frac{1}{2}[1 + \tanh(\bar{\Delta}_r/2T)]$.

According to the discussion, large t_r or small t_r would weaken the suppression of the LZ transition. Thus it is assumed that relaxation will maximally suppress the LZ transition when t_r and τ_r coincide,

$$t_r(v_{\min}) = \tau_r, \quad (23)$$

which leads to a minimum of P_1 at v_{\min} . If only single-phonon absorption is considered within resonance ($|t| \leq \frac{t_r}{2}$), then the system relaxation time τ_r can be estimated by the golden rule with time-averaged energy splitting $\bar{\Delta}_r$ for which

$$\tau_r^{-1} = \pi\alpha \frac{\Delta_0^2}{\bar{\Delta}_r} \exp(-\bar{\Delta}_r/\omega_c) n(\bar{\Delta}_r), \quad (24)$$

where α is the system-bath coupling strength and $n(\bar{\Delta}_r)$ is the Bose-Einstein distribution function. A revisit of the golden rule used in the spin-boson model is given in the Appendix. Comparing Eq. (21) and (24) gives the position of v_{\min} .

Now apply this phenomenological model to our spin-fermion model. Since the system is prepared in the ground state, only absorption can occur if an electron jumps from the left lead to an unoccupied state with lower energy in the right lead. The energy difference of the electron before and after the jump should be Δ_t . The largest energy change by the jump is $\Delta\mu$ (when an electron at the Fermi level in the left lead jump to the Fermi level of the right lead); thus $\Delta_c = \Delta\mu$.

When the sweep velocity v is large for which $t_r \ll \tau_r$, the relaxation can not occur and thus P_1 coincides with P_0 . When the sweep velocity v is small for which $t_r \gg \tau_r$, the system would be fully relaxed according to $\Delta_c = \Delta\mu$ at zero temperature. In the spin-fermion model, the full relaxation of the system is determined not by the temperature but by the chemical potential difference $\Delta\mu$. According to Ref. [56], it has no simple analytical formula for the system polarization $\langle\sigma_z\rangle$, but it is known that $\langle\sigma_z\rangle$ manifests a transition from a fully polarized system, where the system is in the ground state, to an unpolarized system, where $\langle\sigma_z\rangle = 0$ as $\Delta\mu$ increases. Since $\Delta_c = \Delta\mu$, which is equivalent to say $\Delta\mu$ is not large, after fully relaxation the system would be adjusted to the ground state. Therefore $P_1 = 1$ when $v \rightarrow 0$, and this can be seen more clearly from Fig. 3(b) where a larger coupling strength λ accelerates relaxation processes.

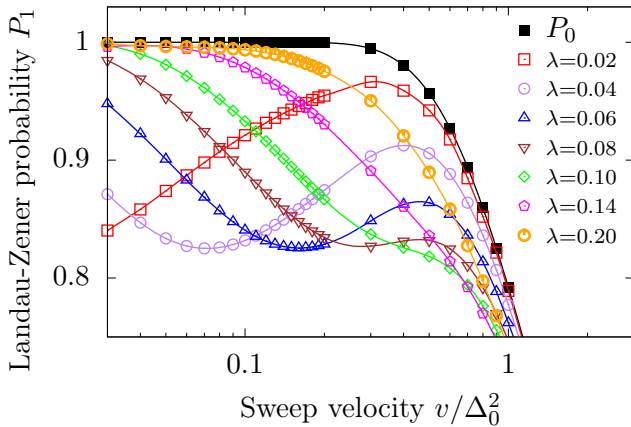


FIG. 4. (Color Online) The LZ probability P_1 versus v for $\Delta\mu = 1.0$ and various λ .

When t_r matches τ_r , the relaxation maximally suppresses the LZ transition, which gives a minimum at v_{\min} . Since the value of $P_1(v_{\min})$ must be smaller than $P_1(v \rightarrow 0) = 1$, as

$v \rightarrow 0$ the probability P_1 must increase again with decreasing v . Therefore P_1 shows a maximum at v_{\max} , and minimum at v_{\min} , and then an increase with decreasing v , as shown in Fig. 2. Basically, the mechanism for nonmonotonic dependence on v in the spin-fermion model is same as that in the spin-boson model. If the system ends up in an unpolarized state with $\langle\sigma_z\rangle = 0$ then we have $P_1 = \frac{1}{2}$. This is the reason why $P_1(v_{\min})$ deviates from P_0 and is closer to $\frac{1}{2}$ for larger $\Delta\mu$, or in other words, larger $\Delta\mu$ would suppress the LZ transition more strongly.

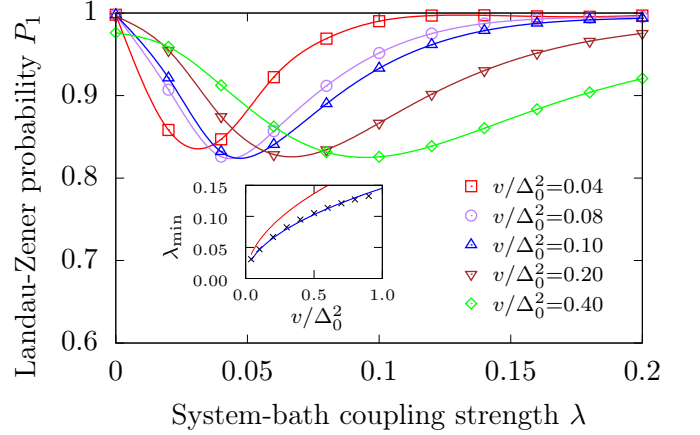


FIG. 5. (Color Online) The LZ probability P_1 versus λ for $\Delta\mu = 1.0$ and various v . Inset: λ_{\min} versus v with same $\Delta\mu$ in the main figure. The simulation data are shown by black dots, results by the phenomenological model are shown by the red line, and the blue line represents a fitting function $y = 0.145x^{1/2}$.

For a fixed time and weak coupling, the decay rate out of the ground state can be estimated by the golden rule if only a single electron jump is considered. After summing up all possible jumps whose energy difference is Δ_t , we obtain the decay rate as (see the Appendix)

$$\tau^{-1} = 2\pi\lambda^2 \frac{\Delta_0^2}{\Delta_t^2} (\Delta\mu - \Delta_t). \quad (25)$$

In the spin-boson model, τ_r^{-1} is archived via simply substituting Δ_t by $\bar{\Delta}_r$ in the expression of τ^{-1} . However, in the spin-fermion model, due to the inverse quadratic dependence on Δ_t of τ^{-1} , it would be more appropriate to estimate τ_r^{-1} by the time-averaged decay rate

$$\begin{aligned} \tau_r^{-1} &= \frac{1}{t_r} \int_{-t_r/2}^{t_r/2} 2\pi\lambda^2 \frac{\Delta_0^2}{\Delta_t^2} (\Delta\mu - \Delta_t) dt \\ &= \frac{4\pi}{vt_r} \lambda^2 \Delta_0^2 \left[\frac{\Delta\mu}{\Delta_0} \operatorname{atan} \left(\frac{vt_r}{2\Delta_0} \right) - \operatorname{asinh} \left(\frac{vt_r}{2\Delta_0} \right) \right]. \end{aligned} \quad (26)$$

This formula predicts that v_{\min} increases almost linearly with increasing $\Delta\mu$ when $\Delta_c \gg \Delta_0$. The positions of v_{\min} versus $\Delta\mu$ for $\lambda = 0.04$ is shown in the inset of Fig. 2. It can be seen that v_{\min} roughly shows a linearly dependence on $\Delta\mu$. However, employing Eq. (23) we have $v_{\min} \approx 0.043\Delta_0^2$ for

$\Delta\mu = 1.0$ and $v_{\min} \approx 0.127\Delta_0^2$ for $\Delta\mu = 2.0$. This result only qualitatively agrees with what is shown in Fig. 2 where $v_{\min} \approx 0.072\Delta_0^2$ for $\Delta\mu = 1.0$ and $v_{\min} \approx 0.087\Delta_0^2$ for $\Delta\mu = 2.0$.

Figure 3 shows the LZ transition probability P_1 versus sweep velocity v for larger λ and various $\Delta\mu$. As seen from Eq. (26), the relaxation rate is proportional to λ^2 for which increasing λ enhances relaxation and decreases τ_r accordingly. For $\lambda = 0.1$ [Fig. 3(a)] the minimum disappears and only a shoulder remains. For $\lambda = 0.2$ [Fig. 3(b)], only a monotonic growth of P_1 with decreasing v remains, and the relaxation processes are greatly accelerated for which at $v/\Delta_0^2 = 0.1$ the LZ transition probabilities P_1 already reduce to 1.

Figure 4 shows the LZ transition probability P_1 versus v for $\Delta\mu = 1.0$ and various λ . For small $\lambda = 0.04, 0.06, 0.08$, the minimum $P_1(v_{\min})$ can be still observed and v_{\min} shifts to larger velocity for increasing λ . The minimum disappears when $\lambda \geq 0.10$ and in this case P_1 goes to 1 for small v . Due to these features, the lines of P_1 in Fig. 4 have cross points, which means there is a nonmonotonic dependence of P_1 on λ . This can be seen more clearly in Fig. 5.

Figure 5 shows the dependence of P_1 on λ for $\Delta\mu = 1.0$ and various v . It can be seen that P_1 shows a minimum at λ_{\min} for a fixed v . Since $t_r^{-1} \propto v$ and $\tau_r^{-1} \propto \lambda^2$, we have $\lambda_{\min}^2 \propto v$ which means there is a simple quadratic dependence between v and λ_{\min} : when v is scaled by a factor of a then λ_{\min} would be scaled by a factor of \sqrt{a} . This conclusion agrees with the results shown in the inset of the figure where a inverse quadratic fitting is shown.

Equation (26) gives a simple description of the effect of λ on τ_r^{-1} , while the effect of $\Delta\mu$ is much more complex. It is because $\Delta\mu$ plays a role as both temperature T and bath cut-off frequency ω_c in the spin-boson model, which makes its effect on the relaxation complex, while larger λ simply enhances the relaxation. In the spin-boson model, it is already mentioned that by the phenomenological picture the behavior of the crossover temperature can be only roughly described with absolute values off by a factor of 3 [44]. This may be the reason why the results of Eq. (26) always have some deviations from simulation data since the effect of ω_c can not be removed from $\Delta\mu$.

B. Results of P_2

Now let us turn to P_2 which stands for the LZ transition probability from down to up state, where the system is prepared in the excited state at $t = -\infty$.

Figure 6 shows the LZ probability P_2 versus v for weak coupling $\lambda = 0.04$ and various $\Delta\mu$. In large sweep velocity regime ($v \gg \Delta_0^2$), since t_r is too short for relaxation P_2 coincides with P_0 , just like P_1 . In the small sweep velocity regime ($v \ll \Delta_0^2$), there is great difference between the behaviors of P_2 and P_1 . For small v , P_1 is close to P_0 , i.e., close to 1, while P_2 is far away from P_0 and close to zero. With fixed $\Delta\mu$ and decreasing v , P_2 shows a maximum at v_{\max} , which is smaller than but close to Δ_0^2 , then decreases all along and no minimum is shown.

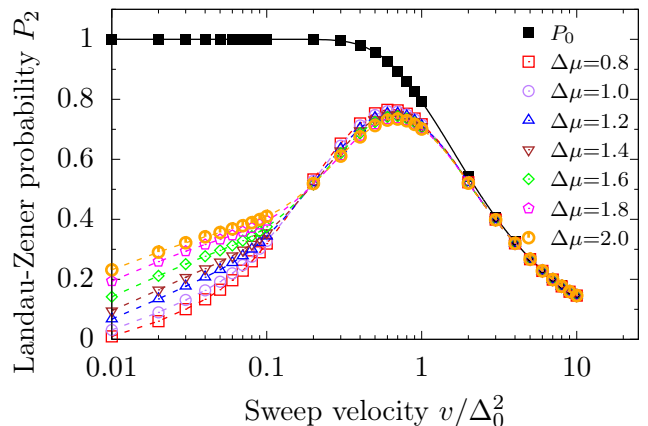


FIG. 6. (Color Online) The LZ probability P_2 versus v for weak system-bath coupling strength $\lambda = 0.04$ and various $\Delta\mu$.

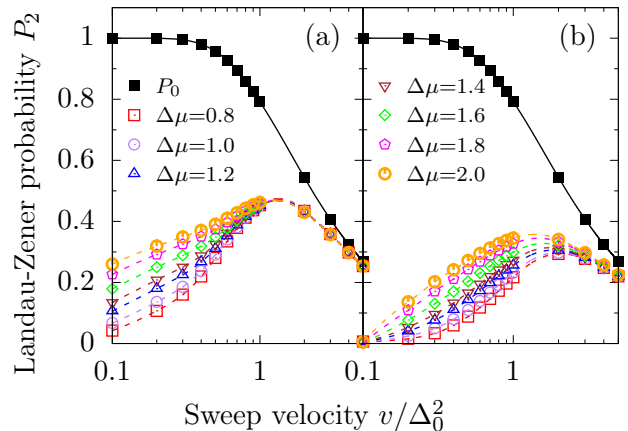


FIG. 7. (Color Online) The same as Fig. 6 for larger system-bath coupling strengths (a) $\lambda = 0.10$ and (b) $\lambda = 0.20$.

Although behaviors of P_1 and P_2 differ greatly for small v , they are due to the same relaxation mechanism. For P_1 , we are seeking the probability of the system to stay in the ground state, while for P_2 , the probability of the system to stay in the excited state is desired. However, when v is small a full relaxation would lead the system towards the ground state, and this makes P_1 go to 1 and P_2 to zero.

There is another difference between the behaviors of P_1 and P_2 in the small- v regime: for P_1 , larger $\Delta\mu$ suppresses the LZ transition probability more strongly, while for P_2 , larger $\Delta\mu$ increases the LZ transition probability instead. This is because, as mentioned earlier, larger $\Delta\mu$ would relax the system toward an unpolarized state, where $\langle\sigma_z\rangle = 0$, which makes P_2 closer to $\frac{1}{2}$. Around v_{\max} , the situation is in another way around for which larger $\Delta\mu$ decreases P_2 . The underlying reason is the same: larger $\Delta\mu$ makes the system go toward an unpolarized state, i.e., makes P_2 closer to $\frac{1}{2}$.

Since the system is initially prepared in the excited state, only emission can occur within resonance ($|t| \leq \frac{t_r}{2}$). In the emission process, there are two kinds jumping: an electron in

the left lead jumps to an unoccupied state with higher energy in the right lead, and an electron in the right lead jumps to an unoccupied state in the left lead with higher energy. The energy difference by the jump should be Δ_t . If only a single electron jump is considered, the golden rule formula for the decay rate out of the excited state is given in the Appendix. Basically, the golden rule states that the decay rate τ^{-1} has a quadratic dependence on λ as in the absorption process, while its dependence on $\Delta\mu$ is of more complexity.

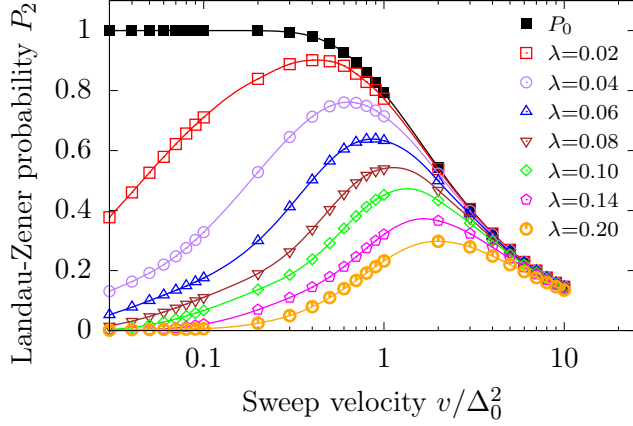


FIG. 8. (Color Online) The LZ probability P_2 versus v for $\Delta\mu = 1.0$ and various λ .

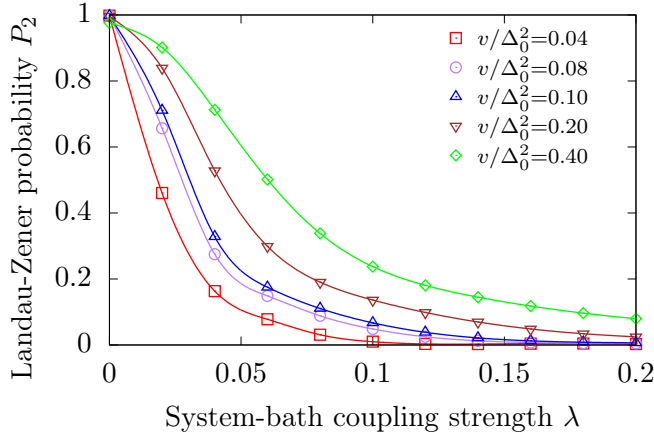


FIG. 9. (Color Online) The LZ probability P_2 versus λ for $\Delta\mu = 1.0$ and various v .

Figure 7 shows the same content as Fig. 6 for larger system-bath coupling strengths. Since the relaxation rate is proportional to λ^2 , larger λ accelerates relaxation and decreases τ_r . It can be seen that with $\Delta\mu = 2.0$ when $\lambda = 0.04$ (Fig. 6) P_2 is close to 0.2 at $v = 0.01\Delta_0^2$, while when $\lambda = 0.1$ [Fig. 7(b)] P_2 is already close to 0.2 at $v = 0.1\Delta_0^2$. For $\lambda = 0.2$ [Fig. 7(b)], P_2 already reduces to zero at $v = 0.1\Delta_0^2$.

Figure 8 shows the LZ transition probability P_2 versus v for $\Delta\mu = 1.0$ and various λ . Unlike P_1 shown in Fig. 4, lines of P_2 in Fig. 8 have no cross points. This is because there is no

v_{\min} in P_2 . In addition, due to the same reason the dependence of λ of P_2 becomes monotonic. This can be seen from Fig. 9 which shows P_2 versus λ for $\Delta\mu = 1.0$ and various v . It can be seen that larger λ accelerates the relaxation and makes P_2 go to zero, and smaller v also enhances the relaxation.

IV. CONCLUSIONS

We have studied LZ transitions in a fermionic environment where a TLS is coupled to two metallic leads kept with different chemical potential at zero temperature. The dynamics of the system is simulated by an iterative numerically exact influence functional path integral method which allows us to include nonadiabatic and non-Markovian effects.

The LZ transition probability is the probability of the system staying in the ground (excited) state P_1 (P_2) after an energy sweep. In the pure LZ problem, the two kinds of probability are symmetric; i.e., they are the same no matter whether the system is initially prepared in the ground or excited state.

The symmetry no longer exists after taking the effect of the environment into consideration. In the large sweep velocity regime, $v \gg \Delta_0^2$, since the resonance time t_r is much shorter than the system relaxation time τ_r , the bath has little influence on the transition; thus both P_1 and P_2 coincide with the pure LZ transition probability P_0 . In the small sweep velocity regime, $v \ll \Delta_0^2$, the system is fully relaxed to the ground state, which makes P_1 go to 1 and P_2 to zero. This is the reason why the symmetry no longer exists. Due to the same reason, P_1 shows a minimum at v_{\min} and λ_{\min} , while P_2 shows no minimum.

According to the phenomenological model, the existence of v_{\min} of P_1 is understood as a nontrivial competition between relaxation and LZ driving, where the LZ transition is maximally suppressed when the resonance time t_r and the system relaxation time τ_r coincide. The system relaxation time τ_r can be estimated by the golden rule, which states that τ_r^{-1} has a quadratic dependence on the system-bath coupling strength λ . This statement agrees with our results, which indicates that the effect of λ is fairly simple.

The effect of $\Delta\mu$ on the dissipation is of more complexity. If we treat $\Delta\mu$ as the temperature, then results similar to those shown in Figs. 2, 3, and 4 can be found in the LZ transitions in the spin-boson model [44]. This is because $\Delta\mu$ can act as a temperature like dephasing contributor. However, it is not really the temperature and the temperature also has its own effect on the LZ transitions. At zero temperature, the system manifests a transition from the ground state to an unpolarized system as $\Delta\mu$ increases. This means that when the value of Δ_t can compare with $\Delta\mu$, then the system would be relaxed to the ground state. Meanwhile in the spin-boson model, the system would not be relaxed to the ground state at finite temperature, and the bath shows no effect on the LZ probability when the system and bath are diagonally coupled at zero temperature [42].

In addition, $\Delta\mu$ also plays the role of the cutoff frequency ω_c of the spin-boson model, where the effect of ω_c can be also only qualitatively described by the phenomenological model.

The dual role of $\Delta\mu$ as both the temperature T and the cut-off frequency ω_c in the spin-boson model makes its effect on the dissipation complex. This may be the reason why results by the phenomenological model always have some deviations from simulation data since the effect of ω_c can not be removed from $\Delta\mu$. The interplay between the external field, system-bath coupling λ and chemical potential difference $\Delta\mu$ remains open for further investigations.

Despite the different effects of the bosonic and fermionic baths discussed above, the phenomenological model also gives some universal predictions despite what kind of environment is present: when the sweep velocity is large, due to small relaxation time window t_r , the effect of the environment can be neglected; when the sweep velocity is small, the system would be fully relaxed according to the environment, where the environment shows its characteristics most; in the intermediate sweep velocity regime, the LZ probability shows a nonmonotonic dependence on the sweep velocity and the coupling parameter. This nonmonotonic feature may be useful for optimal control problems and for further experiments.

Appendix A: Golden Rule

In this appendix, we shall revisit the derivation of the golden rule formula used for the LZ transition in the spin-boson model [44], and then following the same spirit we shall derive the golden rule for the spin-fermion model studied in this article.

1. Spin-Boson Model

The Hamiltonian of the spin-boson model is

$$H = H_S + H_B + H_{SB}, \quad (\text{A1})$$

where the system and bath Hamiltonian are

$$H_S = \frac{\varepsilon}{2}\sigma_z + \frac{\Delta_0}{2}, \quad H_B = \sum_k \omega_k b_k^\dagger b_k. \quad (\text{A2})$$

Here ε and Δ_0 are level splitting and tunneling amplitude of the TLS, respectively, and b_k (b_k^\dagger) are bosonic annihilation (creation) operators. For simplicity we assume ε is positive. The system-bath coupling is written as

$$H_{SB} = \frac{\sigma_z}{2} \sum_k \lambda_k (b_k + b_k^\dagger), \quad (\text{A3})$$

and the bath influence is described by the spectral density

$$J(\omega) = \sum_k \lambda_k^2 \delta(\omega - \omega_k) = 2\alpha\omega \exp(-\omega/\omega_c), \quad (\text{A4})$$

where an Ohmic form with cutoff frequency ω_c and coupling strength α is considered.

The system Hamiltonian H_S can be diagonalized by an unitary rotation for which

$$\bar{H}_S = e^{\frac{1}{2}i\theta\sigma_y} H_S e^{-\frac{1}{2}i\theta\sigma_y} = \frac{1}{2}\Delta_t\sigma_z \quad (\text{A5})$$

when $\tan\theta = \Delta_0/\varepsilon$, where $\Delta_t = \sqrt{\varepsilon^2 + \Delta_0^2}$. After the rotation, the system-bath coupling becomes

$$\bar{H}_{SB} = \frac{1}{2\Delta_t}(\varepsilon\sigma_z - \Delta_0\sigma_x) \sum_k \lambda_k (b_k + b_k^\dagger). \quad (\text{A6})$$

The Pauli matrix σ_x can be written in terms of $\sigma_+ = \frac{1}{2}(\sigma_x + i\sigma_y)$ and $\sigma_- = \frac{1}{2}(\sigma_x - i\sigma_y)$ for which $\sigma_x = \sigma_+ + \sigma_-$. If only a single phonon absorption is considered in the absorption process, then in \bar{H}_{SB} only the term $\frac{1}{2}\frac{\Delta_0}{\Delta_t}\sum_k \sigma_+ b_k$ is relevant. Let $|1\rangle$ denote the excited state ($\sigma_z = +1$) and $|2\rangle$ denote the ground state ($\sigma_z = -1$), and let $|n_k\rangle$ denote the phonon state $\frac{1}{\sqrt{n_k!}}(b_k^\dagger)^{n_k}|0\rangle$, where $|0\rangle$ is the vacuum state. Then starting from the state $|2\rangle$, the probability $p(t)$ of the system to go to the state $|1\rangle$ at time t is given by the golden rule formula [1, 2]

$$p(t) = \frac{1}{4} \frac{\Delta_0^2}{\Delta_t^2} \int_0^t \int_0^t \sum_k \rho_k \lambda_k^2 e^{i(\Delta_t - \omega_k)(t_1 - t_2)} \times |\langle 1|\sigma_+|2\rangle \langle n_k - 1|b_k|n_k\rangle|^2 dt_1 dt_2, \quad (\text{A7})$$

where ρ_k is the Gibbs distribution function

$$\rho_k = \exp\left(-\frac{n_k\omega_k}{T}\right) / \sum_{n_k} \exp\left(-\frac{n_k\omega_k}{T}\right) \quad (\text{A8})$$

with temperature T . If the integrand in Eq. (A7) dies sufficiently fast as a function of $(t_1 - t_2)$, then the decay rate of the system out of the state $|2\rangle$ can be defined as

$$\begin{aligned} \tau^{-1} &= \frac{1}{4} \frac{\Delta_0^2}{\Delta_t^2} \int_{-\infty}^{\infty} \sum_k \lambda_k^2 e^{i(\Delta_t - \omega_k)t} n(\omega_k) dt \\ &= \frac{1}{4} \frac{\Delta_0^2}{\Delta_t^2} \sum_k 2\pi \lambda_k^2 \delta(\Delta_t - \omega_k) n(\omega_k) \\ &= \pi\alpha \frac{\Delta_0^2}{\Delta_t} \exp(-\Delta_t/\omega_c) n(\Delta_t), \end{aligned} \quad (\text{A9})$$

where $n(\omega) = (e^{\beta\omega} - 1)^{-1}$ is the Bose-Einstein distribution function.

Similarly, if only a single phonon emission is considered in the emission process then in \bar{H}_{SB} only the term $\frac{1}{2}\frac{\Delta_0}{\Delta_t}\sum_k \sigma_- b_k^\dagger$. Therefore the decay rate of the system out of the state $|1\rangle$ is

$$\tau^{-1} = \pi\alpha \frac{\Delta_0^2}{\Delta_t} \exp(-\Delta_t/\omega_c) [1 + n(\Delta_t)]. \quad (\text{A10})$$

From Eq. (A9) and (A10) it can be seen that at zero temperature the decay rate out of the ground state is zero, while the decay rate out of the excited state remains finite, as they should be.

2. Spin-Fermion Model

In the spin-fermion model, for a fixed time t , denoting vt in Eq. (2) by ε yields

$$H_S = \frac{\varepsilon}{2}\sigma_z + \frac{\Delta_0}{2}\sigma_x. \quad (\text{A11})$$

For simplicity, we assume ε is positive. This H_S can be diagonalized by the same rotation as in Eq. (A5). Let $\Delta_t = \sqrt{\varepsilon^2 + \Delta_0^2}$; then after the rotation the system-bath coupling becomes

$$\bar{H}_{SB} = \frac{1}{\Delta_t} \sum_{\alpha\beta; kq} V_{\alpha\beta} (\varepsilon\sigma_z - \Delta_0\sigma_x) c_{\alpha k}^\dagger c_{\beta q}. \quad (\text{A12})$$

Similarly, we can write σ_x in terms of σ_+ and σ_- as $\sigma_x = \sigma_+ + \sigma_-$. In the absorption process, if only a single electron jump is considered then only jumps from the left lead to an unoccupied state with lower energy in the right lead are permitted. The energy difference of the electron before and after jump should be Δ_t . Therefore in \bar{H}_{SB} only the term $\frac{1}{\Delta_t} \sum_{kq} V_{RL} \sigma_+ c_{Rq}^\dagger c_{Lk}$ is relevant, and the golden rule formula for the decay rate of the system out of the ground state can be written as

$$\tau^{-1} = 2\pi\lambda^2 \frac{\Delta_0^2}{\Delta_t^2} (\Delta\mu - \Delta_t) \quad (\text{A13})$$

for $\Delta_t \leq \Delta\mu$. When $\Delta_t > \Delta\mu$, the decay rate becomes zero; thus we have $\Delta_c = \Delta\mu$.

The situation is more complex in the emission process. Two kinds jumping are allowed: an electron in the left lead jumps

to an unoccupied state with higher energy in the right lead (the term $\frac{1}{\Delta_t} \sum_{kq} V_{RL} c_{Rk}^\dagger c_{Lq}$ in \bar{H}_{SB} is involved), and an electron in the right lead jumps to an unoccupied state in the left lead (the term $\frac{1}{\Delta_t} \sum_{kq} V_{LR} c_{Lk}^\dagger c_{Rq}$ in \bar{H}_{SB} is involved). The energy difference before and after the jump should be Δ_t . After summing up all possible jumps, the decay rate in the former jump can be identified as

$$\tau^{-1} = 2\pi\lambda^2 \frac{\Delta_0^2}{\Delta_t^2} \Delta\mu \quad (\text{A14})$$

for $\Delta_0 \leq \Delta_t \leq \frac{1}{2}(D - \Delta\mu)$ and

$$\tau^{-1} = 2\pi\lambda^2 \frac{\Delta_0^2}{\Delta_t^2} \left[\frac{1}{2}(D + \Delta\mu) - \Delta_t \right] \quad (\text{A15})$$

for $\frac{1}{2}(D - \Delta\mu) < \Delta_t \leq \frac{1}{2}(D + \Delta\mu)$. The decay rate in the latter jump is

$$\tau^{-1} = 2\pi\lambda^2 \frac{\Delta_0^2}{\Delta_t^2} (\Delta_t - \Delta\mu) \quad (\text{A16})$$

for $\Delta\mu < \Delta_t \leq D$. The decay rate becomes zero under other conditions; therefore $\Delta_c = D$.

-
- [1] A. J. Leggett, S. Chakravarty, A. T. Dorsey, M. P. A. Fisher, A. Garg, and W. Zwerger, *Reviews of Modern Physics* **59**, 1 (1987).
- [2] U. Weiss, *Quantum Dissipative Systems* (World Scientific, Singapore, 1993).
- [3] F. Hund, *Zeitschrift fur Physik* **43**, 805 (1927).
- [4] J. R. Oppenheimer, *Physical Review* **31**, 66 (1928).
- [5] L. D. Landau, *Physikalische Zeitschrift der Sowjetunion* **2**, 46 (1932).
- [6] C. Zener, *Proceedings of the Royal Society A* **137**, 696 (1932).
- [7] E. Stückelberg, *Helvetica Physica Acta* **5**, 369 (1932).
- [8] E. Majorana, *Nuovo Cimento* **9**, 43 (1932).
- [9] V. May and O. Kühn, *Charge and Energy Transfer Dynamics in Molecular Systems* (Wiley-VCH verlag, Berlin, 2011).
- [10] A. Thiel, *Journal of Physics G: Nuclear and Particle Physics* **16**, 867 (1990).
- [11] D. A. Harmin and P. N. Price, *Physical Review A* **49**, 1933 (1994).
- [12] W. Xie and W. Domcke, *The Journal of Chemical Physics* **147**, 184114 (2017).
- [13] M. Sillanpää, T. Lehtinen, A. Paila, Y. Makhlin, and P. Hakonen, *Physical Review Letters* **96**, 187002 (2006).
- [14] D. M. Berns, M. S. Rudner, S. O. Valenzuela, K. K. Berggren, W. D. Oliver, L. S. Levitov, and T. P. Orlando, *Nature* **455**, 51 (2008).
- [15] H. DeRaedt, S. Miyashita, K. Saito, D. García-Pablos, and N. García, *Physical Review B* **56**, 11761 (1997).
- [16] W. Wernsdorfer, *Science* **284**, 133 (1999).
- [17] R. J. C. Spreeuw, N. J. van Druten, M. W. Beijersbergen, E. R. Eliel, and J. P. Woerdman, *Physical Review Letters* **65**, 2642 (1990).
- [18] D. Bouwmeester, N. H. Dekker, F. E. v. Dorsselaer, C. A. Schrama, P. M. Visser, and J. P. Woerdman, *Physical Review A* **51**, 646 (1995).
- [19] D. Witthaut, E. M. Graefe, and H. J. Korsch, *Physical Review A* **73**, 063609 (2006).
- [20] A. Zenesini, H. Lignier, G. Tayebirad, J. Radogostowicz, D. Ciampini, R. Mannella, S. Wimberger, O. Morsch, and E. Arimondo, *Physical Review Letters* **103**, 090403 (2009).
- [21] A. J. Olson, S.-J. Wang, R. J. Niffenegger, C.-H. Li, C. H. Greene, and Y. P. Chen, *Physical Review A* **90**, 013616 (2014).
- [22] J. Ankerhold and H. Grabert, *Physical Review Letters* **91**, 016803 (2003).
- [23] A. Izmalkov, M. Grajcar, E. Il'ichev, N. Oukhanski, T. Wagner, H.-G. Meyer, W. Krech, M. H. S. Amin, A. M. van den Brink, and A. M. Zagorskin, *Europhysics Letters* **65**, 844 (2004).
- [24] M. Wubs, K. Saito, S. Kohler, Y. Kayanuma, and P. Hänggi, *New Journal of Physics* **7**, 218 (2005).
- [25] W. D. Oliver, Y. Yu, J. C. Lee, K. K. Berggren, L. S. Levitov, and T. P. Orlando, *Science* **310**, 1653 (2005).
- [26] L. F. Wei, J. R. Johansson, L. X. Cen, S. Ashhab, and F. Nori, *Physical Review Letters* **100**, 113601 (2008).
- [27] G. D. Fuchs, G. Burkard, P. V. Klimov, and D. D. Awschalom, *Nature Physics* **7**, 789 (2011).
- [28] A. V. Shytov, D. A. Ivanov, and M. V. Feigel'man, *The European Physical Journal B* **36**, 263 (2003).
- [29] A. Izmalkov, S. H. W. van der Ploeg, S. N. Shevchenko, M. Grajcar, E. Il'ichev, U. Hübner, A. N. Omelyanchouk, and H.-G. Meyer, *Physical Review Letters* **101**, 017003 (2008).
- [30] S. Shevchenko, S. Ashhab, and F. Nori, *Physics Reports* **492**, 1 (2010).
- [31] P. Neilinger, S. N. Shevchenko, J. Bogár, M. Rehák, G. Oel-sner, D. S. Karpov, U. Hübner, O. Astafiev, M. Grajcar, and E. Il'ichev, *Physical Review B* **94**, 094519 (2016).

- [32] A. Chatterjee, S. N. Shevchenko, S. Barraud, R. M. Otxoa, F. Nori, J. J. L. Morton, and M. F. Gonzalez-Zalba, *Physical Review B* **97**, 045405 (2018).
- [33] Z. Wang, W. C. Huang, Q. F. Liang, and X. Hu, *Scientific Reports* **8**, 7920 (2018).
- [34] Y. Kayanuma, *Journal of the Physical Society of Japan* **53**, 108 (1984).
- [35] M. Grifoni and P. Hänggi, *Physics Reports* **304**, 229 (1998).
- [36] C. Wittig, *The Journal of Physical Chemistry B* **109**, 8428 (2005).
- [37] Y. Gefen, E. Ben-Jacob, and A. O. Caldeira, *Physical Review B* **36**, 2770 (1987).
- [38] P. Ao and J. Rammer, *Physical Review Letters* **62**, 3004 (1989).
- [39] P. Ao and J. Rammer, *Physical Review B* **43**, 5397 (1991).
- [40] Y. Kayanuma and H. Nakayama, *Physical Review B* **57**, 13099 (1998).
- [41] H. Kobayashi, N. Hatano, and S. Miyashita, *Physica A: Statistical Mechanics and its Applications* **265**, 565 (1999).
- [42] M. Wubs, K. Saito, S. Kohler, P. Hänggi, and Y. Kayanuma, *Physical Review Letters* **97**, 200404 (2006).
- [43] K. Saito, M. Wubs, S. Kohler, Y. Kayanuma, and P. Hänggi, *Physical Review B* **75**, 214308 (2007).
- [44] P. Nalbach and M. Thorwart, *Physical Review Letters* **103**, 220401 (2009).
- [45] R. S. Whitney, M. Clusel, and T. Ziman, *Physical Review Letters* **107**, 210402 (2011).
- [46] P. Haikka and K. Mølmer, *Physical Review A* **89**, 052114 (2014).
- [47] L. Arceci, S. Barbarino, R. Fazio, and G. E. Santoro, *Physical Review B* **96**, 054301 (2017).
- [48] Z. Huang and Y. Zhao, *Physical Review A* **97**, 013803 (2018).
- [49] D. E. Makarov and N. Makri, *Chemical Physics Letters* **221**, 482 (1994).
- [50] N. Makri, *Journal of Mathematical Physics* **36**, 2430 (1995).
- [51] S. Weiss, J. Eckel, M. Thorwart, and R. Egger, *Physical Review B* **77**, 195316 (2008).
- [52] D. Segal, A. J. Millis, and D. R. Reichman, *Physical Review B* **82**, 205323 (2010).
- [53] P. Nozières and C. T. D. Dominicis, *Physical Review* **178**, 1097 (1969).
- [54] T.-K. Ng, *Physical Review B* **51**, 2009 (1995).
- [55] T.-K. Ng, *Physical Review B* **54**, 5814 (1996).
- [56] D. Segal, D. R. Reichman, and A. J. Millis, *Physical Review B* **76**, 195316 (2007).
- [57] R. Chen and X. Xu, *Physical Review B* **100**, 115437 (2019).
- [58] D. E. Makarov and N. Makri, *Physical Review E* **52**, 5863 (1995).
- [59] D. E. Makarov and N. Makri, *Physical Review B* **52**, R2257 (1995).
- [60] N. Makri and L. Wei, *Physical Review E* **55**, 2475 (1997).
- [61] N. Makri, *The Journal of Chemical Physics* **106**, 2286 (1997).
- [62] D. Segal, A. J. Millis, and D. R. Reichman, *Physical Chemistry Chemical Physics* **13**, 14378 (2011).
- [63] L. Simine and D. Segal, *The Journal of Chemical Physics* **138**, 214111 (2013).
- [64] D. Segal, *Physical Review B* **87**, 195436 (2013).
- [65] B. K. Agarwalla and D. Segal, *The Journal of Chemical Physics* **147**, 054104 (2017).
- [66] N. Makri, *The Journal of Chemical Physics* **111**, 6164 (1999).